

NASA/TM-2002-210787



Major Element Analyses of the Target Rocks at Meteor Crater, Arizona

*Thomas H. See
Lockheed-Martin Space Operations
Houston, Texas*

*Friedrich Hörz and David W. Mittlefehldt
NASA Johnson Space Center
Houston, Texas*

*Laura Varley
Lunar and Planetary Institute
Houston, Texas*

*Stan Mertzman
Franklin & Marshall College
Lancaster, Pennsylvania*

*David Roddy
United States Geological Survey
Flagstaff, Arizona*

THE NASA STI PROGRAM OFFICE . . . IN PROFILE

Since its founding, NASA has been dedicated to the advancement of aeronautics and space science. The NASA Scientific and Technical Information (STI) Program Office plays a key part in helping NASA maintain this important role.

The NASA STI Program Office is operated by Langley Research Center, the lead center for NASA's scientific and technical information. The NASA STI Program Office provides access to the NASA STI Database, the largest collection of aeronautical and space science STI in the world. The Program Office is also NASA's institutional mechanism for disseminating the results of its research and development activities. These results are published by NASA in the NASA STI Report Series, which includes the following report types:

- **TECHNICAL PUBLICATION.** Reports of completed research or a major significant phase of research that present the results of NASA programs and include extensive data or theoretical analysis. Includes compilations of significant scientific and technical data and information deemed to be of continuing reference value. NASA's counterpart of peer-reviewed formal professional papers but has less stringent limitations on manuscript length and extent of graphic presentations.
- **TECHNICAL MEMORANDUM.** Scientific and technical findings that are preliminary or of specialized interest, e.g., quick release reports, working papers, and bibliographies that contain minimal annotation. Does not contain extensive analysis.
- **CONTRACTOR REPORT.** Scientific and technical findings by NASA-sponsored contractors and grantees.
- **CONFERENCE PUBLICATION.** Collected papers from scientific and technical conferences, symposia, seminars, or other meetings sponsored or cosponsored by NASA.
- **SPECIAL PUBLICATION.** Scientific, technical, or historical information from NASA programs, projects, and mission, often concerned with subjects having substantial public interest.
- **TECHNICAL TRANSLATION.** English-language translations of foreign scientific and technical material pertinent to NASA's mission.

Specialized services that complement the STI Program Office's diverse offerings include creating custom thesauri, building customized databases, organizing and publishing research results . . . even providing videos.

For more information about the NASA STI Program Office, see the following:

- Access the NASA STI Program Home Page at <http://www.sti.nasa.gov>
- E-mail your question via the Internet to help@sti.nasa.gov
- Fax your question to the NASA Access Help Desk at (301) 621-0134
- Telephone the NASA Access Help Desk at (301) 621-0390
- Write to:
NASA Access Help Desk
NASA Center for AeroSpace Information
7121 Standard
Hanover, MD 21076-1320

NASA/TM-2002-210787



Major Element Analyses of the Target Rocks at Meteor Crater, Arizona

*Thomas H. See
Lockheed-Martin Space Operations
Houston, Texas*

*Friedrich Hörz and David W. Mittlefehldt
NASA Johnson Space Center
Houston, Texas*

*Laura Varley
Lunar and Planetary Institute
Houston, Texas*

*Stan Mertzman
Franklin & Marshall College
Lancaster, Pennsylvania*

*David Roddy
United States Geological Survey
Flagstaff, Arizona*

Lyndon B. Johnson
Space Center
National Aeronautics and
Space Administration

August 2002

Acknowledgements

We greatly appreciate the support by D. Barringer and J. Shoemaker and their staff of the Meteor Crater Enterprises, Inc., Flagstaff, Arizona. Their participation made for pleasurable fieldwork. L. Varley gratefully acknowledges support for the XRD investigations by the Summer Intern Program of the Lunar and Planetary Institute, Houston, Texas.

Dedication

This report is dedicated to our co-author Dr. David J. Roddy (1932-2002), United States Geological Survey, Flagstaff, Arizona. David was an unselfish supporter of all Meteor Crater studies and he last climbed the walls of his beloved crater during the collection of this sample suite. We will remember him fondly as a respected colleague and dear friend who made profound contributions to the basic understanding of impact processes.

Available from:

NASA Center for AeroSpace Information
7121 Standard
Hanover, MD 21076-1320

National Technical Information Service
5285 Port Royal Road
Springfield, VA 22161

This report is also available in electronic form at <http://techreports.larc.nasa.gov/cgi-bin/NTR>

Contents

	Page
ABSTRACT	1
INTRODUCTION	2
Procedures and Methods.....	3
Field Procedures	3
XRF Analysis.....	5
XRD Analyses	6
Results.....	6
Bulk Composition	6
Modal Composition.....	7
Examples of Data Utilization	9
Target Rocks and Impact Melts.....	9
CO ₂ Loss From Carbonates During Hypervelocity Impact	11
Conclusions	12
References	14

Table

Table 1. Composition of individual stratigraphic subsections at Meteor Crater and average compositions of the major geologic formations.....	18
---	----

Figures

Figure 1. Summary plot of the major element concentrations, normalized to a volatile-free basis, of the target rocks at Meteor Crater, AZ.....	19
Figure 2. Correlation plot of CaO + MgO versus total loss-on-ignition (LOI) for the 12 Kaibab samples summarized in Table 1.....	20
Figure 3. Modal content (wt %) of quartz in the Kaibab Formation at Meteor Crater, AZ, based on XRD studies	21
Figure 4. Comparison of the measured SiO ₂ , MgO, and CaO contents (wt %) of 12 Kaibab subsections based on XRF and comparison with stoichiometric calculations using the modal abundance of quartz and dolomite from XRD.	22
Figure 5. Comparison of the major-element composition of the target rocks and impact melts at Meteor Crater, AZ.....	23

ABSTRACT

We collected ~ 400 rock chips in continuous vertical profile at Meteor Crater, Arizona, representing—from bottom to top—the Coconino, Toroweap, Kaibab, and Moenkopi Formations. These rock chips were subsequently pooled into 23 samples for compositional analysis by X-ray fluorescence methods, each sample reflecting a specific stratigraphic “subsection” ~ 5-10 m thick. In addition, the modal abundance of quartz, dolomite, and calcite was determined for the entire Kaibab Formation at vertical resolutions of 1-2 meters using 57 samples. The purpose of these investigations was to support ongoing compositional analyses of the impact melts and their stratigraphic source depth(s) and other studies at Meteor Crater that depend on the composition of the target rocks.

The Coconino Formation comprises the lower half of the crater cavity, from ~ 90 m below the original target surface to the bottom of the crater. It is an exceptionally pure sandstone composed of > 97 wt % SiO₂. The Toroweap is only 2 m thick and compositionally similar to Coconino; therefore, it is not a good compositional marker horizon. The Kaibab Formation, ~ 80 m thick, is highly variable in SiO₂, MgO, and CaO. On a CO₂-free basis, the average Kaibab contains 53 wt % SiO₂, 16 wt % MgO, and 26 wt % CaO. X-ray diffraction studies show that the Kaibab Formation at Meteor Crater is dominated by dolomite and quartz, albeit in highly variable proportions; calcite is a minor phase at best. The Kaibab at Meteor Crater is therefore a sandy dolomite rather than a limestone, consistent with pronounced facies changes in the Permian of southeast Arizona over short vertical and horizontal distances. The Moenkopi forms the 12-m-thick cap rock and is a calcareous silt that has the highest Al₂O₃ (~ 7.5 wt %) and FeO (~ 4 wt %) concentrations of all target rocks.

With several examples, we illustrate how this systematic compositional and modal characterization of the target lithologies may contribute to an understanding of Meteor Crater, such as the depth of its melt zone, and to impact cratering in general, such as the liberation of CO₂ from shocked carbonates.

INTRODUCTION

Detailed compositional characterization of impact melts from a large number of terrestrial craters revealed that these melts are remarkably intimate and homogeneous mixtures of the prevalent country rocks (e.g., Dence, 1971; Grieve et al., 1977; Phinney et al., 1977; Engelhardt, 1997). Obviously, the stratigraphic-structural relationships of the precursor rocks must be understood at dimensional scales much smaller than that of the total melt volume in order to evaluate the relative contributions of specific target strata to these melts and to reconstruct the total extent of a crater's melt zone, including melt depth. This cannot be accomplished with great precision in most terrestrial craters because of their advanced erosional state or because they occurred in structurally complex, igneous or metamorphic terrains. As a consequence, the specific stratigraphic source depths of most impact melts are not well known and remain poorly defined, even for such well-studied cases as the Ries (e.g., Engelhardt, 1997). This constrains the utility of extraterrestrial impact melts as probes for planetary stratigraphy and crustal composition (e.g., Ryder 1990; Spudis, 1993).

Furthermore, a detailed understanding of target stratigraphy is necessary for the numerical modeling of impact events. Associated algorithms are continuously advancing and modern hydrocodes can accommodate targets composed of layers with distinctly different physical and/or compositional properties (e.g., Pierazzo and Melosh, 2000). In addition, the so-called analytical equations of state (ANEOS) are being increasingly used in such hydrocode calculations (Melosh, 2000). These ANEOS are constructs that are based on the measured oxide concentrations of the rocks to be simulated, and they replace the equations of state measured on specific rock-specimens. Any reference library of the shock properties of specific rocks is limited and may not contain high-fidelity analogues for any specific event. Thus, detailed compositional and mineralogical characterization of individual target strata allows for the synthesis of high-fidelity equations of state and, consequently, for possible improvements of current hydrocode models.

The 1-km-diameter Meteor Crater in Arizona ranks among the best-preserved impact structures on Earth and exposes a structurally simple, initially flat-lying sedimentary stratigraphy in its exposed walls. By studying the deformations and displacements of these sediments, Shoemaker (1960 and 1963) established—in a series of classical studies—the basic principles of the shock-induced material motions during hypervelocity impact. The observations of additional field studies of Meteor

Crater summarized in Roddy (1978) form the basis for detailed hydrocode calculations by Roddy et al. (1980) or Schnabel et al. (1999).

Accordingly, Meteor Crater is the archetype for small, bowl-shaped impact structures. Larger, structurally more complex craters are believed to result from the gravitational collapse of their transient cavities. The latter have also relatively simple, bowl-shaped geometries, because the shock-induced material motions are substantially identical for all craters (Croft, 1985; Grieve et al., 1989; Melosh, 1989; Melosh and Ivanov, 1999). Since melt formation is associated with the amplitude of the initial shock wave, most melting will take place during early cratering stages, before transient cavity collapse, even for large structures. It is possible, therefore, that a detailed understanding of the melt-forming processes in small bowl-shaped craters, such as Meteor Crater, will have general applications at larger crater scales as well (e.g., Cintala and Grieve, 1998).

Most of the existing investigations of the impact melts at Meteor Crater (Nininger, 1954, Brett, 1967, Kelly et al., 1974, Morgan et al., 1975) addressed the meteoritic component of these melts and it was not until recently that possible relationships of melts and target rocks were being addressed (e.g., Kargel et al., 1996, Hörz et al., 2002). To place these ongoing melt investigations or future hydrocode modeling and other studies at Meteor Crater into suitable lithologic and stratigraphic context, it seemed necessary to systematically determine the composition and mineralogy of the target rocks, with emphasis on the dominant, yet highly variable Kaibab Formation. This paper describes such analyses using X Ray Fluorescence (XRF) and X-Ray Diffraction (XRD) methods.

Procedures and Methods

Field Procedures

The target rocks at Meteor Crater include, from the bottom, the Coconino, Toroweap, and Kaibab Formations, all of Permian age, and the Triassic Moenkopi Formation as detailed by McKee (1938), Shoemaker (1960), Shoemaker and Kieffer (1974), and Roddy (1978). Kieffer (1971) studied the petrographic and compositional characteristics of the Coconino Formation in exemplary detail. However, the dominant Kaibab Formation, ~ 80 m thick, remains poorly characterized compositionally, as does the Moenkopi Formation (~ 10 m thick). These strata are significant because they compose the upper half of the ~ 180-m-deep crater. We note that McKee (1938)

describes substantial, regional facies changes of the Kaibab Formation in southeast Arizona due to a near littoral environment that was characterized by repeated transgressions and regressions of the Permian Sea, and by the precipitation of either calcite or dolomite and by variable admixtures of clastic quartz. Shoemaker (1960) and Shoemaker and Kieffer (1974) report substantial lithological variety within the Kaibab at Meteor Crater, such as sandstones and dolomites.

We accomplished the sampling of representative rocks in the exposed walls at Meteor Crater during three separate traverses, each optimized for the collection of the Coconino, Kaibab, and Moenkopi Formations, respectively. Vertical distance from sample to sample was measured via yardstick and tape, rather than theodolite. All samples were freshly dislodged. Typical sampling interval of the “field samples” (i.e., the contents of a single sampling bag) was 1-2 meters; most bags contained 3-5 fragments taken at still smaller intervals. Obviously, we sampled lithologically distinct layers as small as 20 cm individually. We labeled individual field samples/bags by absolute elevation above the lowermost sampling station, which was a few meters above the present crater floor. Each bag weighed approximately 1 kg.

Traverse I was devoted to the oldest strata, Coconino and Toroweap, taking advantage of a large, ~ 80-m-wide, slump block in the east-southeast corner of the crater. Major gullies on either side of this block cut through the omnipresent talus and expose the deepest levels of the Coconino within the entire crater (Shoemaker, 1960). Nevertheless, this block represents only the uppermost 35 m of the Coconino Formation and the transient cavity bottom is estimated to be an additional 50-60 m below the sampled section (Roddy, 1978; Grieve et al., 1989). Traverse I also includes a complete section of the Toroweap Formation, ~ 1.6 m thick, as well as of the lowermost Kaibab.

Traverse II was dedicated to the collection of Kaibab. It started ~ 40 m above the crater floor, due north of the centrally located mine shaft. Unfortunately, the Toroweap/Kaibab contact at this location is buried under talus, as is typical for the exposed walls, but Traverse II started in the massive stratum that was already sampled at the end of Traverse I, thereby ensuring stratigraphic continuity. The traverse angled generally in a north-northwest direction toward the major trail (i.e., Old Mule Trail) that leads from the rim to the crater floor. It intersected this trail ~ 90 m above the crater floor, and followed the trail to the well-exposed Moenkopi/Kaibab contact. The trail itself follows a major thrust fault in the crater’s northwest corner, but we collected all the samples of Traverse II on the east side of the fault to ensure stratigraphic integrity.

Traverse III was dedicated to collection of the Moenkopi Formation and was located ~ 250 m west of the museum building, where a stratigraphically complete, 12-m-thick section is exposed. This section is substantially upturned and it is actually folded on itself as part of the overturned rim flap (Shoemaker, 1960).

We collected 115 sample bags (containing ~ 400 individual chips) in this manner: 35 from the Coconino, 7 from the Toroweap, 57 from the Kaibab, and 16 from the Moenkopi. This sampling strategy resulted in approximately one sample bag per meter of vertical section. Toroweap and Moenkopi were sampled at especially high resolutions consistent with their potential roles as important, compositional marker horizons.

XRF Analysis

Available resources allowed for ~20-25 bulk analyses via XRF; this limitation mandated that individual field samples be pooled. Throughout this paper, we will refer to such pooled samples as stratigraphic “subsections,” the latter typically combining some 2-5 sample bags; such subsections are typically 5-10 m in vertical extent, depending on lithologic homogeneity. Pooling the field samples into subsections accounted for the stratigraphic significance of each sample bag as follows:

- Step 1: Dislodged centimeter-sized samples from every rock chip in a sample bag to make each collection interval and “field sample” as representative as possible. Total mass generated in this manner was typically ~ 10-15 g per bag; all was ground and passed through a 1-mm sieve.
- Step 2: Generated stratigraphic “subsections” by pooling these < 1-mm powders of individual sample bags. Each bag contributed to the pooled mix in weighted proportions commensurate with its vertical sampling interval relative to that of the entire subsection. Assuming invariant sample density, this thickness-related weighting ensured that the contribution of each field sample corresponded to its stratigraphic significance.
- Step 3: Thoroughly homogenized these stratigraphically weighted powders of < 1 mm grain size, ground them to < 63 μm , and analyzed them via XRF methods as described in Boyd and Mertzmann (1987).

The pooling of 115 field samples resulted in 23 subsections (4 Coconino, 2 Toroweap, 12 Kaibab, and 5 Moenkopi). Obviously, most boundaries of these newly

generated subsections were predicated by field observations, accounting for lithological boundaries, yet some of the boundaries were arbitrary (e.g., in the homogeneous Coconino sandstone or in some massive sections of Kaibab).

XRD Analyses

We performed XRD analyses only on Kaibab samples, employing aliquots of the < 1-mm fractions generated for each field sample/sample bag as described in Step 1 above. This material was ground to < 63 μm , as were all standard materials. These standards consisted of ground single-crystal quartz, calcite, and dolomite mixed in known weight proportions. We also added a fixed amount of Al_2O_3 powder as an internal standard to these mixtures, to monitor possible variances of the diffractometer patterns related to sample preparation and possible differences in the intensity and detailed geometry of the incident X-ray beam. We used a Scintag XDS 2000 diffractometer in combination with a copper ceramic tube run at 45 kV potential and 40 mA tube current. We scanned over an angular range of 20-60° 2 θ at a scan rate of 1 degree/minute. Consistent with the compositional data shown in Figures 1 & 2, most Kaibab samples did not reveal measurable quantities of calcite in the XRD patterns, at most 5%. As a result, we only compared the Kaibab samples to standards made from powdered quartz and dolomite, rather than the three-phase mixtures.

Results

Bulk Composition

Table 1 shows the results of the XRF analyses. The loss-on-ignition (LOI) component largely reflects CO_2 and approaches 40 wt % in the most carbonate-rich rocks. Figure 1 summarizes the major-element concentrations on a volatile-free basis. All analyses of Coconino yield > 96 wt % SiO_2 and are rather invariant otherwise, suggesting that Coconino is a pure and compositionally homogeneous sandstone, as already described by others (e.g., Kieffer, 1971). The lowest Toroweap sample is very similar to the Coconino with minimally elevated MgO, yet its upper section seems transitional to Kaibab. The compositional affinity to either Coconino or Kaibab, coupled with the thinness of this unit, indicates that Toroweap will not be a diagnostic tracer of stratigraphy in the impact melts of Meteor Crater.

Even the most cursory inspection of the 12 Kaibab analyses reveals unexpectedly high SiO_2 and MgO for each individual analysis, as well as for the formation as a whole, which is commonly referred to as a "limestone" (e.g., Shoemaker, 1960; Roddy, 1978).

Significantly, the Kaibab Formation contains variable, yet copious amounts of quartz, with SiO_2 varying from 30%-70%. Neighboring subsections—on vertical scales of a few meters—may differ greatly from each other, but there is no systematic, compositional trend as a function of stratigraphic position within the Kaibab. The Kaibab Formation at Meteor Crater obviously reflects a very sandy facies and appears to be dominated throughout by dolomite rather than calcite, judging from the abundance of MgO relative to CaO in every single analysis.

The latter point is emphasized in Figure 2, which plots measured CaO + MgO versus total LOI for comparison with stoichiometrically ideal dolomite and calcite. The surprisingly constant correlation of CaO + MgO versus LOI in Figure 2 suggests that the carbonate component of the Kaibab is substantially invariant throughout. This invariant behavior either reflects a mixture of stoichiometrically ideal dolomite and minor calcite in precisely constant proportions throughout the entire formation, or it reflects a modestly Ca-enriched dolomite, the latter having ~ 54 mol % CaO.

Returning to Figure 1, the Moenkopi Formation is obviously not as pure a sandstone as the Coconino, with typical $\text{SiO}_2 < 70$ wt % in the Moenkopi. The elevated Al_2O_3 and Fe_2O_3 render the Moenkopi the most Al- and Fe-rich material at Meteor Crater. The Moenkopi also contains modest calcite and has a high CaO/MgO ratio (on average ~ 10), that differs from that of the Kaibab which typically has CaO/MgO < 2.

Table 1 and Figure 1 also present the averaged compositions of each major formation at Meteor Crater. These averages were calculated in a fashion analogous to step 2 above by weighting the compositions of specific subsections in proportion to their thickness relative to that of the entire formation. As a consequence, the averages are as representative as possible, considering that individual rock chips were dislodged at vertical intervals of < 1 m.

Modal Composition

The substantial heterogeneity among diverse Kaibab subsections suggests potentially large lithologic variability at small, vertical scales. Some of these variabilities are obvious in the field, such as thin layers almost completely composed of sand. As a consequence, we employed XRD methods to obtain the modal abundances of the major rock-forming minerals, quartz, dolomite, and calcite. In all, 56 field samples were collected from the Kaibab Formation.

The XRD data confirm that the Kaibab Formation is completely dominated by quartz and dolomite. Figure 3 summarizes the modal abundance of quartz, with dolomite being the complementary component. A surprisingly large number of samples yield essentially only quartz, with dolomite barely detectable at a level of < 5%. In addition, there is a large variability on a sample-by-sample basis and there is no systematic correlation of the quartz/dolomite ratio and overall stratigraphic position within the Kaibab. However, systematic changes in the quartz content may be inferred for specific stratigraphic intervals, such as a decreasing sand component for the 49- to 58-m (from base) section; conversely, systematically increasing quartz contents applies the 74- to 85-m section. These obviously reflect periods of decreasing or increasing continental contributions to the evolving marine sediments.

The absence or paucity of calcite is somewhat surprising for the Kaibab Formation. To further test the general validity of the XRD results illustrated in Figure 3, we converted the observed modal abundances of quartz and (ideally) stoichiometric dolomite into absolute concentrations of SiO₂, CaO, and MgO for each subsection; these stoichiometrically derived oxide concentrations may then be compared with the XRF measurements as shown in Figure 4. The agreement between the two data sets is good, although not perfect. With one exception, the XRD analyses systematically overestimate the SiO₂ content by ~ 5-15 wt % relative to the XRF values. We have no ready explanation for this discrepancy, but it could be associated with systematically different grain sizes at scales < 63 μm between the natural samples and our standard powders produced from large single crystals. The agreement would be better if we had used a Ca-rich dolomite as suggested by Figure 3, instead of ideally stoichiometric dolomite. Nevertheless, we refrained from pursuing the detailed causes of this discrepancy, as they seem to be of little consequence for the modal characterization of the Kaibab Formation as a sandy dolomite.

The apparent absence of calcite and total dominance of dolomite in both the XRF and XRD analyses was unexpected, because Kaibab is typically referred to as limestone at Meteor Crater. Although modal analysis via XRD methods is not very precise, there simply is very little pure calcite present in these rocks — at most 5% in a few samples. The stoichiometric arguments illustrated in Figure 2 strongly support this conclusion. There is no discrete stratum at vertical scales of meters at Meteor Crater that contains abundant calcite and that would represent pure limestone.

The classification of the Kaibab as “limestone” reflects the dominant facies of the Kaibab Formation in central and southeast Arizona, but it is incorrect for Meteor Crater.

Substantial facies changes are common over relatively short lateral and vertical distances (McKee, 1938) and the Kaibab at the Meteor Crater site happens to be totally dominated by dolomite. Shoemaker (1960, 1963) and Shoemaker and Kieffer (1974) clearly recognized the dominance of dolomite and the existence of individual sandstone layers in the local Kaibab; the above lithological details did not matter for their structural field investigations and descriptions of cratering motions. Nevertheless, we recommend that the Kaibab Formation at Meteor Crater be referred to as a sandy dolomite in the future.

The near-shore depositional environment of Kaibab described by McKee (1938) allows for arbitrary mixtures of detrital quartz and carbonate precipitates during repeated transgressions and regressions of the Permian Sea. The apparently systematic increase or decrease of the quartz content over relatively small stratigraphic intervals that is observed in Figure 3 seems to reflect such cyclic behavior.

Examples of Data Utilization

Target Rocks and Impact Melts

The impact melts at Meteor Crater occur as millimeter- to centimeter-sized objects on and beyond the crater rim. They have regular (spherical, ellipsoid, etc.) and highly irregular shapes, all suggestive of finely dispersed melt spray (Nininger, 1954). The impactor was a class IAB iron meteorite (Buchwald, 1975) and the melts contain high concentrations of disseminated projectile (Brett, 1967; Kelly et al., 1974; Morgan et al., 1975). Interestingly, until recently the actual melts and their relationship to target rocks were not studied in any great detail (Mittlefehldt et al., 1992; Kargel et al., 1996; See et al., 1999). A summary of the most recent electron microprobe analyses of the melts is illustrated in Figure 5, from Hörz et al., 2002. This plot normalizes all melt and rock compositions to the principal target components, SiO₂, CaO, and MgO, reflecting the dominant minerals (quartz, dolomite, and calcite, respectively) that constitute > 95% of the target rocks. The dashed line represents a linear mixing line between Ca-rich Kaibab dolomite and pure quartz. The summary figure illustrates average compositions of the major target formations and of specific subsections based on XRF, as well as the average composition of individual melt specimen, based on electron microprobe analysis. It is obvious that the melts/glasses have affinities to the target rocks, yet the respective mixes of target rocks contributing to specific melts seem highly variable. This seems rather unusual for impact melts that are commonly of very restricted compositional range (e.g., Grieve et al., 1977; Phinney et al., 1977, Engelhardt, 1997),

suggesting rather intimate and complete mixing of target rocks. The melts at Meteor Crater are compositionally variable and their composition clusters in three major groups; the latter are furthermore manifested by meteoritic contamination, such as total FeO and NiO, the Fe/Ni ratio, as well as their crystallization products as detailed by Hörz et al., 2002.

Returning to Figure 5, the dominant group of melts falls on the mixing line between Kaibab-dolomite and quartz, yet all of these melts have higher SiO₂ than the average Kaibab. This suggests either that additional quartz was derived from the Coconino Formation, or that the melts originated predominantly from select, quartz-rich sections of the Kaibab, such as the uppermost 15-20 m (sections K_j - K_l in Figure 1) or some more deep-seated Kaibab strata (K_a - K_f). None of the melts approach, compositionally, the dolomite-rich composition of the middle parts of the Kaibab Formation, such as subsections K_g or K_i. This major melt group can actually be subdivided into two subgroups on the basis of their dolomite contents and other characteristics. The melts of low-dolomite content crystallize pyroxene only, while the other subgroup crystallizes pyroxene + olivine. Both groups contain uniformly high FeO (> 20 wt %), but the melts of high-dolomite content contain unfractionated Fe/Ni, whereas the other subgroup contains fractionated Fe/Ni (see Hörz et al., 2002).

Returning to Figure 5, the third group of melts falls off the dolomite-quartz mixing line and contains substantial quantities of Moenkopi. The latter melts also contain uniformly low meteoritic contaminants (< 10 wt % FeO), all of unfractionated Fe/Ni. Obviously these Moenkopi-rich and meteorite-poor melts derive from shallower source depth than the Kaibab-rich melts, the latter possibly even containing Coconino-derived quartz from depth > 90 m.

To quantify the mixing relationships illustrated in Figure 5, which are based on only three elements, Hörz et al. (2002) employed the weighted, least square mixing program MIXER (Korotev et al., 1995) utilizing all oxides listed in Table 1, except TiO₂ and P₂O₅, which were not available for the melts. These mixing calculations also included the projectile, an apparently major component judging from the FeO content of the melts relative to the target rocks. These calculations revealed that the “shallow” melts are composed of ~ 55% (weight) Moenkopi, 40% Kaibab, and 5% meteorite. Unfortunately, the mixing calculations cannot resolve whether the excess SiO₂ relative to average Kaibab is caused by the addition of Coconino sandstone or by quartz-rich Kaibab. The mixing calculations seem compatible with melt depths < 30 m utilizing the quartz-rich K_j, K_k, and K_l strata, or with melt depth > 90 m, utilizing average Kaibab and as much as

12% Coconino sandstone. Intermediate melt depths seem excluded, because the dolomite-rich strata, such as the K_g and K_i subsections (see Figure 1) do not contain enough SiO_2 to produce the observed melts. The “deep-seated” melts derive either from the quartz-rich rocks above the K_i stratum, or from a combination of the entire Kaibab and modest Coconino sandstone. At present, neither scenario can be excluded.

CO₂ Loss From Carbonates During Hypervelocity Impact

Impact into carbonate-bearing targets and excessive pollution of the atmosphere by shock-liberated CO₂ may lead to severe, if not catastrophic, environmental crises, such as the KT event (e.g., Pope et al., 1997 or Pierazzo et al., 1998). However, the subject of shock-induced devolatilization of carbonates is somewhat controversial because the minimum shock pressures for the onset of devolatilization of calcite or dolomite are poorly defined (e.g., Lange and Ahrens, 1986; Ivanov and Deutsch, 2002; Skala et al., 2002). Furthermore, there is observational evidence from the Houghton Dome crater, Devon Island, Canada (Martinez et al., 1994), that the refractory residue of carbonates will re-combine rapidly with shock-liberated CO₂; Langenhorst et al. (2000) verify the nearly instantaneous production of secondary carbonates in experimentally shocked calcite at > 70 GPa. In a recent summary of these and other natural and experimental observations, Agrinier et al. (2001) postulate that such “back reactions” are sufficiently efficient to trap most CO₂, thereby keeping it from entering the atmosphere. Obviously, such back reactions may greatly diminish the role of CO₂ as an atmospheric pollutant during KT-like impacts. Our new analyses of the target rocks at Meteor Crater combined with the above melt studies specifically illustrate that these melts represent the volatile depleted residues of carbonates. The Ca-rich nature of the dolomite is clearly preserved in the CaO/MgO ratio of the melts (e.g., Figure 4). In addition, optical investigations of the melts reveal no secondary carbonates. Thermal gravimetric analyses of the melts (Morris, personal communications, 2002) in combination with IR-spectroscopic characterization of the evolved gases revealed the presence of H₂O; neither CO nor CO₂ was observed during these thermal gravimetric analysis runs. Because we did not observe secondary carbonates or any CO₂ in the glass, all volatiles must have escaped the growing crater cavity. Thus, CO₂ loss is rather prominent and seemingly efficient at Meteor Crater. The observations of Martinez et al. (1994) at the Houghton Dome most likely relate to the rare occasion where CO₂ became physically trapped in some void space, affording sufficient time to react with the refractory carbonate residue. Secondary calcite seems rare at Houghton Dome and the sample analyzed by Martinez et al. (1994) may not be typical. Finally, the calcite specimen of

Langenhorst et al. (2000) was embedded in a steel container during the actual shock experiments; any liberated gas was not allowed to escape, thus the products of back reactions.

We conclude that CO₂ will interact with its own refractory residue only if trapped and confined. This seems to be a rare occurrence. The more typical fate of shock-liberated CO₂ during natural impacts is to escape into the atmosphere as initially suggested by Kieffer and Simonds (1980) or Lange and Ahrens (1986). In the case of large-scale impacts, such as the KT-event, it may well produce sufficiently severe pollution of the atmosphere to precipitate an environmental crisis of global proportions that will lead, ultimately, to the observed mass extinctions (Pope et al., 1997; Pierazzo et al., 1998).

Conclusions

We collected representative target rocks at Meteor Crater, Arizona, and analyzed them compositionally via XRF and modally via XRD methods. Consistent with previous studies (e.g., McKee, 1938; Kieffer, 1971), we found that the Coconino Formation is a pure sandstone and its composition is essentially invariant over a vertical distance of 35 m and most likely over still greater depths. The minor Toroweap, ~ 1.5 m thick, is transitional to the Kaibab Formation. Kaibab is ~ 80 m thick and dominates the upper portions of the target. The local Kaibab is a sandy dolomite that exhibits highly variable quartz/dolomite ratios, including almost pure sandstones; calcite is present in minor proportions at best; the traditional summary term of “limestone” should be abandoned. The uppermost Moenkopi Formation, ~ 10 m thick, is composed of calcareous silts that have substantially higher CaO/MgO ratios than the Kaibab and that contain more Al₂O₃ and FeO than any other target rock at Meteor Crater.

The distinct lithologic and compositional differences between the three major stratigraphic units seem suited for the investigation of detailed melt-mixing process at Meteor Crater and to evaluate the stratigraphic extent of the crater's melt zone with unprecedented fidelity, a potential that is very rare among terrestrial craters. In addition, the target rocks contain relatively little FeO, and most FeO observed in the impact melts must have been derived from the impactor (e.g., Ninninger, 1954; Morgan et al., 1975). This opens the possibility of investigating the mixing of projectile and target melts within a stratigraphic context (e.g., Hörz et al., 2002). Unfortunately, the unexpectedly heterogeneous composition of the melts at Meteor Crater, combined with the high SiO₂ concentration of the average Kaibab, results in somewhat ambiguous assignments of melt depth at Meteor Crater. It is entirely possible that most

melts are indeed the volatile-depleted residue of only the Kaibab Formation, as postulated by Kargel et al. (1996), but modest contributions from the Coconino sandstone may not be excluded positively at present. The improved lithological and compositional characterization of the target rocks will benefit high-fidelity numerical models of the Meteor Crater impact, however (e.g., Melosh, 2000), and such improved calculations should provide additional insight on the depth of melting.

Lastly, quantification of the total content of carbonates in the target will assist in evaluating total CO₂ production during the Meteor Crater event; an important subject that relates to environmental crises and mass extinctions associated with large-scale hypervelocity impact impacts, such as the KT event (Pierazzo et al., 1998; Agrinier et al., 2001).

These considerations render the compositional characterization of the target rocks at Meteor Crater as a timely endeavor.

REFERENCES

- Agrinier P., Deutsch A., Schaerer U., and Martinez I. (2001) Fast back-reactions of shock-released CO₂ from carbonates: An experimental approach. *Geochim. Cosmochim. Acta*, **65**, 2615-2632.
- Brett R. (1967) Metallic spherules in impactite and tektite glasses. *Amer. Mineral.*, **52**, 721-733.
- Boyd F.R. and Mertzman S.A. (1987) Composition of structure of the Kaapvaal lithosphere, southern Africa. In *Magmatic Processes – Physiochemical Principles*, (ed. B.O. Mysen). The Geochemical Society, Special Publication **1**, pp. 13-24.
- Buchwald R.V. (1975) *Handbook of Iron Meteorites*. Univ. California Press, Berkeley, CA, 1418p.
- Cintala M.J. and Grieve R.A.F. (1998) Scaling impact-melt and crater-dimensions: implications for the lunar cratering record. *Met. Planet. Sci.*, **33**, 889-912.
- Croft S. K. (1985) The scaling of complex craters. *LPSC15th, J. Geophys. Res.*, **90**, C828-C842.
- Dence M.R. (1971) Impact melts. *J. Geophys. Res.*, **76**, 5552-5565.
- Engelhardt W.v. (1997) Suevite Breccia of the Ries impact crater, Germany: Petrography, chemistry, and shock metamorphism of crystalline rock clasts, *Met. Planet. Sci.*, **32**, 545-554.
- Grieve R.A.F., Dence M.R., and Robertson P.B. (1977) Cratering processes: As interpreted from the occurrence of impact melts. In *Impact and Explosion Cratering* (eds. D.J. Roddy, R.O. Pepin, and R.S. Merrill), pp. 791-814. Pergamon Press, New York, NY, USA.
- Grieve R.A.F., Garvin J.B., Coderre J.M., and Ruppert J. (1989) Test of a geometric model for the modification stage of simple impact crater development. *Meteoritics*, **24**, 83-88.
- Hörz F., See T.H., Galindo C., and Mittlefehldt D.W. (2002) Petrographic studies of the impact melts from Meteor Crater, AZ. *Met. Planet. Science*, **37**, 501-531.
- Ivanov B.A. and Deutsch A. (2002) The phase diagram of CaCO₃ in relation to shock compression and decomposition. *Physics Earth Planet. Interiors*, **129**, 131-143.
- Kargel J.S., Coffin P., Kraft M., Lewis J., Moore C.B., Roddy D.J., Shoemaker E.M., and Wittke J.H. (1996) Systematic collection and analysis of meteoritic materials from Meteor Crater, AZ. *Lunar Planet. Sci.*, **XXVII**, 645-646 (Abstract).

- Kelly W.R., Holdsworth E., and Moore C.B. (1974) The chemical composition of metallic spheroids and metallic particles within impactite from Barringer Meteorite Crater, Arizona. *Geochim. Cosmochim Acta*, **38**, 533-544.
- Kieffer S.W. (1971) Shock metamorphism of the Coconino Sandstone at Meteor Crater, Arizona. *J. Geophys. Res.*, **76**, 5449-5473.
- Kieffer, S.W. and Simonds, C.H. (1980) The role of volatiles and the lithology in the impact cratering process. *Rev. Geophys. Space Physics*, **18**, 143-181.
- Korotev R.L., Haskin L. A., and Jolliff B.L. (1995) A simulated geochemical rover mission to the Taurus Littrow valley of the Moon. *J. Geophys. Res.*, **100**, 14403-14420.
- Lange M.A. and Ahrens T.J. (1986) Shock-induced CO₂ loss from CaCO₃: implications for early planetary atmospheres. *Earth Planet. Sci. Lett.*, **83**, 1-15.
- Langenhorst F., Deutsch A., Ivanov B.A., and Hornemann U. (2000) On the shock behavior of CaCO₃: dynamic loading and fast unloading experiments – modeling mineralogical observations. In *Lunar Planet. Sci. XXXI, Lunar Planetary Institute CD ROM*, Abstract # 1851.
- Martinez I., Agrinier P., Schaerer U., and Javoy M. (1994) A SEM-ATEM and stable isotope study of carbonates from the Haughton impact crater, Canada. *Earth. Planet. Sci. Lett.*, **121**, 559-574.
- McKee E.D. (1938) The environment and history of the Toroweap and Kaibab Formations of northern Arizona and southern Utah. *Carnegie Inst. Washington Pub.*, **492**, 221 pp.
- Melosh H.J. (1989) *Impact Cratering: a Geologic Process*, Oxford Univ. Press, New York, 245 pp.
- Melosh H.J. (2000) A new and improved equation of state for impact computations. *Lunar. Planet. Sci. XXXI*, 1903 (Abstract).
- Melosh H.J. and Ivanov B.A. (1999) Impact crater collapse. *Ann. Rev. Earth Planet. Sci.*, **27**, 385-415.
- Mittlefehldt D.W., See T.H., and Hörz F. (1992) Projectile dissemination in impact melts from Meteor Crater, AZ. *Lunar Planet. Sci. XXVIII*, 919-920 (Abstracts).
- Morgan J. W., Higuchi H., Ganapathy R., and Anders E. (1975) Meteoritic material in four terrestrial meteorite craters. *Proc. Lunar Sci. Conf.* **6th**, 1609-1623.
- Nininger H.H. (1954) Impactite slag at Barringer Crater. *Am. J. Sci.*, 277-290.

- Phinney W.C. and Simonds C.H. (1977) Dynamical applications of the petrology and distribution of impact melt rocks. In *Impact and Explosion Cratering*, D.J. Roddy et al., eds., Pergamon Press, 117-130.
- Pierazzo, E. and Melosh H.J. (2000) Understanding oblique impacts from experiments, observations and modeling. *Ann. Rev. Earth. Planet. Sci.*, **28**, 147-167.
- Pierazzo E., Kring D.A., and Melosh H.J. (1998) Hydrocode simulation of the Chixculub impact event and the production of climatically active gases. *J. Geophys. Res.*, **103**, E9, 28, 607-625.
- Pope K.O., Baines K.H., Ocampo A.C., and Ivanov B.A. (1997) Energy, volatile production, and climatic effects of the Chixculub Cretaceous/Tertiary impact. *J. Geophys. Res.*, **102**, E9, 21, 645-664.
- Roddy D.J. (1978) Pre-impact geological conditions, physical properties, energy calculations, meteorite and initial dimensions and orientation of joints, faults, and walls at Meteor Crater, Arizona. *Proc. Lunar Planet. Sci. Conf.* **9th**, 3891-3930.
- Roddy D.J., Schuster S. H., Kreyenhagen K.N., and Orphal D. L. (1980) Computer code calculations of the formation of Meteor Crater, Arizona: Calculations MC-1 and MC-2. *Proc. Lunar Planet. Sci. Conf.* **11th**, 2275-2308.
- Ryder G. (1990) Lunar Samples, lunar accretion, and the early bombardment of the Moon. *EOS, Trans. Amer. Geophys. Union*, **71**, 313-330.
- Schnabel C., Pierazzo E., Xue S, Herzog G.F., Masarik J., Cresswell R.G., Di Tada M.L., Liu. K., and Fifield L.K. (1999) Shock melting of Canyon Diablo impactor: Constraints from nickel 59 measurements and numerical modeling. *Science*, **285**, 85-88.
- See T.H., Galindo C., Yang V., Mittlefehldt D., and Hörz F. (1999) Major-element composition of ballistically dispersed melts from Meteor Crater, AZ. *Lunar Planet. Sci. XXX*, 1633 (Abstracts).
- Shoemaker E.M. (1960) Penetration mechanics of high velocity meteorites, illustrated by Meteor Crater, Arizona. *Internat. Geol. Con*, **21st**, 418-434.
- Shoemaker E.M. (1963) Impact mechanics at Meteor Crater, Arizona. In *The Moon, Meteorites and Comets* (eds. B. M. Middlehurst and G. P. Kuiper), pp. 301-306. Univ. Chicago Press (Chicago, Illinois).
- Shoemaker E.M. and Kieffer S.W. (1974) Guidebook to the Geology of Meteor Crater. *Center for Meteorite Studies, Arizona State Univ., Tempe, AZ*, 66 pp.

Skala R., Ederova J., Matojka P., and Hörz F. (2002) Mineralogical investigations of experimentally shocked dolomite: implications for the outgassing of carbonates. *GSA Special Paper XXX*, Koeberl, C. ed., in press, 2002.

Spudis, P. (1993) The Geology of Multi-Ring Impact Basins. *Cambridge Planetary Science Series 8*, 263 pp.

Table 1. Composition of individual stratigraphic subsections at Meteor Crater and average compositions of the major geologic formations. (C=Coconino; T=Toroweap, K=Kaibab; M=Moenkopi; individual samples are labeled a-x, with “a” representing the most deeply seated sample within a given formation.) “Thickness” refers to individual subsections, while “cumulative thickness” refers to total sampling depth below the original target surface. LOI = loss on ignition. All data are reported in weight percent.

	Cumulative		SiO ₂	TiO ₂	Al ₂ O ₃	Fe ₂ O ₃	FeO	MnO	MgO	CaO	Na ₂ O	K ₂ O	P ₂ O ₅	LOI	Total
	Thickness (meters)	Thickness (meters)													
M_e	3.1	3.1	58.62	0.42	7.45	2.63	0.10	0.07	1.10	13.69	0.03	1.44	0.12	13.65	99.32
M_d	1.9	5.0	60.68	0.37	8.31	2.86	0.30	0.08	1.43	11.43	0.03	1.54	0.12	12.60	99.75
M_c	2.1	7.1	65.58	0.47	9.11	2.62	0.31	0.05	0.83	8.69	0.02	1.67	0.13	10.08	99.56
M_b	2.1	9.2	65.36	0.46	8.28	2.01	0.23	0.05	0.98	9.64	0.02	1.45	0.12	10.90	99.50
M_a	3.1	12.3	74.60	0.43	6.11	0.77	0.14	0.04	0.73	7.23	0.01	1.12	0.09	8.26	99.53
K_l	6.1	18.4	46.10	0.19	2.76	1.41	0.48	0.06	8.85	16.34	0.02	0.70	0.11	22.76	99.78
K_k	4.7	23.1	34.24	0.12	2.15	0.08	0.58	0.03	12.68	20.38	0.04	0.59	0.10	28.98	99.97
K_j	5.2	28.3	38.45	0.11	1.89	0.00	0.57	0.02	11.80	19.33	0.02	0.51	0.15	27.05	99.90
K_i	7.6	35.9	16.36	0.07	1.20	0.00	0.68	0.02	16.21	27.14	0.05	0.27	0.10	38.17	100.27
K_h	5.6	41.5	44.35	0.12	2.00	0.00	0.44	0.02	10.54	17.05	0.03	0.62	0.08	24.68	99.93
K_g	6.1	47.6	17.83	0.06	0.84	0.23	0.17	0.02	16.12	27.44	0.05	0.27	0.08	37.43	100.54
K_f	6.7	54.3	40.95	0.13	2.21	0.06	0.33	0.03	10.81	18.56	0.03	0.59	0.28	26.04	100.02
K_e	6.1	60.4	40.35	0.13	2.31	0.11	0.22	0.03	11.01	18.76	0.03	0.56	0.25	26.11	99.87
K_d	6.4	66.8	40.81	0.13	2.17	0.19	0.27	0.03	11.10	18.37	0.03	0.53	0.27	26.06	99.96
K_c	5.4	72.2	57.43	0.16	2.84	0.00	0.24	0.02	7.48	12.14	0.02	0.70	0.28	18.28	99.59
K_b	6.8	79.0	37.30	0.12	1.94	0.00	0.34	0.04	12.00	19.58	0.04	0.45	0.22	28.08	100.11
K_a	6.3	85.3	52.15	0.14	2.26	0.00	0.34	0.04	9.02	14.25	0.01	0.48	0.37	20.58	99.64
T_b	0.8	86.1	90.85	0.09	2.31	0.24	0.06	0.01	1.38	1.75	0.00	0.46	0.07	3.20	100.42
T_a	0.6	86.7	96.67	0.07	1.64	0.12	0.11	0.00	0.22	0.17	0.00	0.28	0.05	0.72	100.05
C_d	8.6	95.3	96.99	0.05	1.45	0.05	0.11	0.00	0.08	0.15	0.00	0.17	0.02	0.55	99.62
C_c	8.9	104.2	97.54	0.04	1.10	0.03	0.11	0.00	0.02	0.09	0.00	0.13	0.02	0.38	99.46
C_b	8.4	112.6	96.55	0.12	1.90	0.12	0.10	0.00	0.09	0.12	0.00	0.22	0.04	0.62	99.88
C_a	8.5	121.1	97.03	0.07	1.53	0.02	0.16	0.00	0.05	0.13	0.00	0.23	0.03	0.50	99.75
Formation	Cumulative		SiO ₂	TiO ₂	Al ₂ O ₃	Fe ₂ O ₃	FeO	MnO	MgO	CaO	Na ₂ O	K ₂ O	P ₂ O ₅	LOI	Total
	Thickness (meters)	Thickness (meters)													
Moenkopi	12.3	12.3	65.30	0.43	7.67	2.63	1.88	0.06	0.99	10.17	0.02	1.42	0.11	11.05	99.10
Kaibab	73	85.3	38.32	0.12	2.02	2.05	0.16	0.03	11.57	19.31	0.03	0.51	0.19	27.29	99.57
Toroweap	1.4	86.7	93.34	0.08	2.02	0.73	0.17	0.01	0.88	1.07	0.00	0.38	0.06	2.14	100.16
Coconino	34.4	121.1	97.03	0.07	1.49	0.67	0.05	0.00	0.06	0.12	0.00	0.19	0.03	0.51	99.55

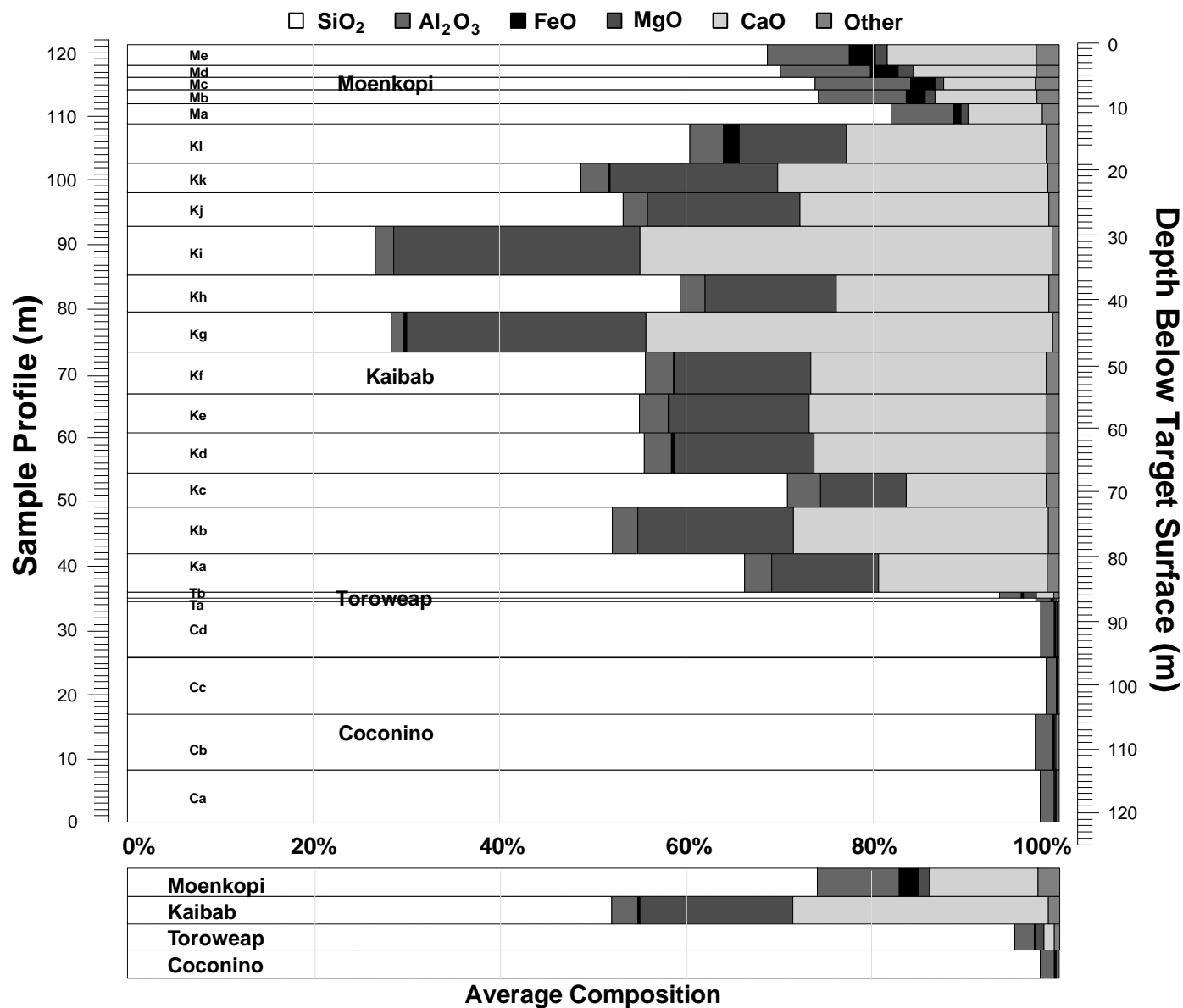


Figure 1. Summary plot of the major element concentrations, normalized to a volatile-free basis, of the target rocks at Meteor Crater, AZ. Each analysis represents an average of some 15-25 individual rock chips that were sampled at vertical intervals < 1 m. Also illustrated are the average compositions for the major stratigraphic formations. (bottom insert).

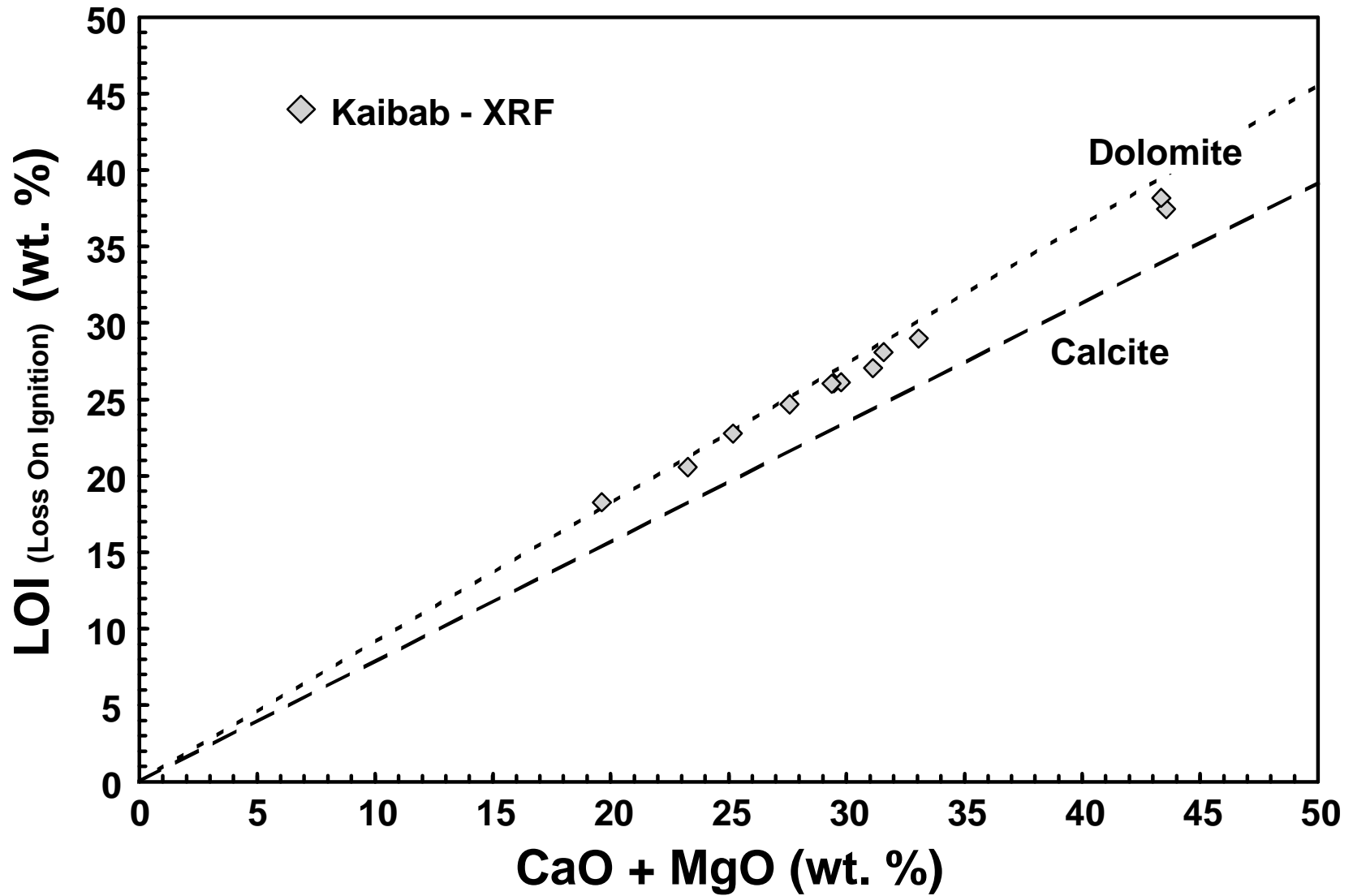


Figure 2. Correlation plot of CaO + MgO versus total loss-on-ignition for the 12 Kaibab samples summarized in Table 1. Also included are the correlation lines of stoichiometrically ideal dolomite and calcite.

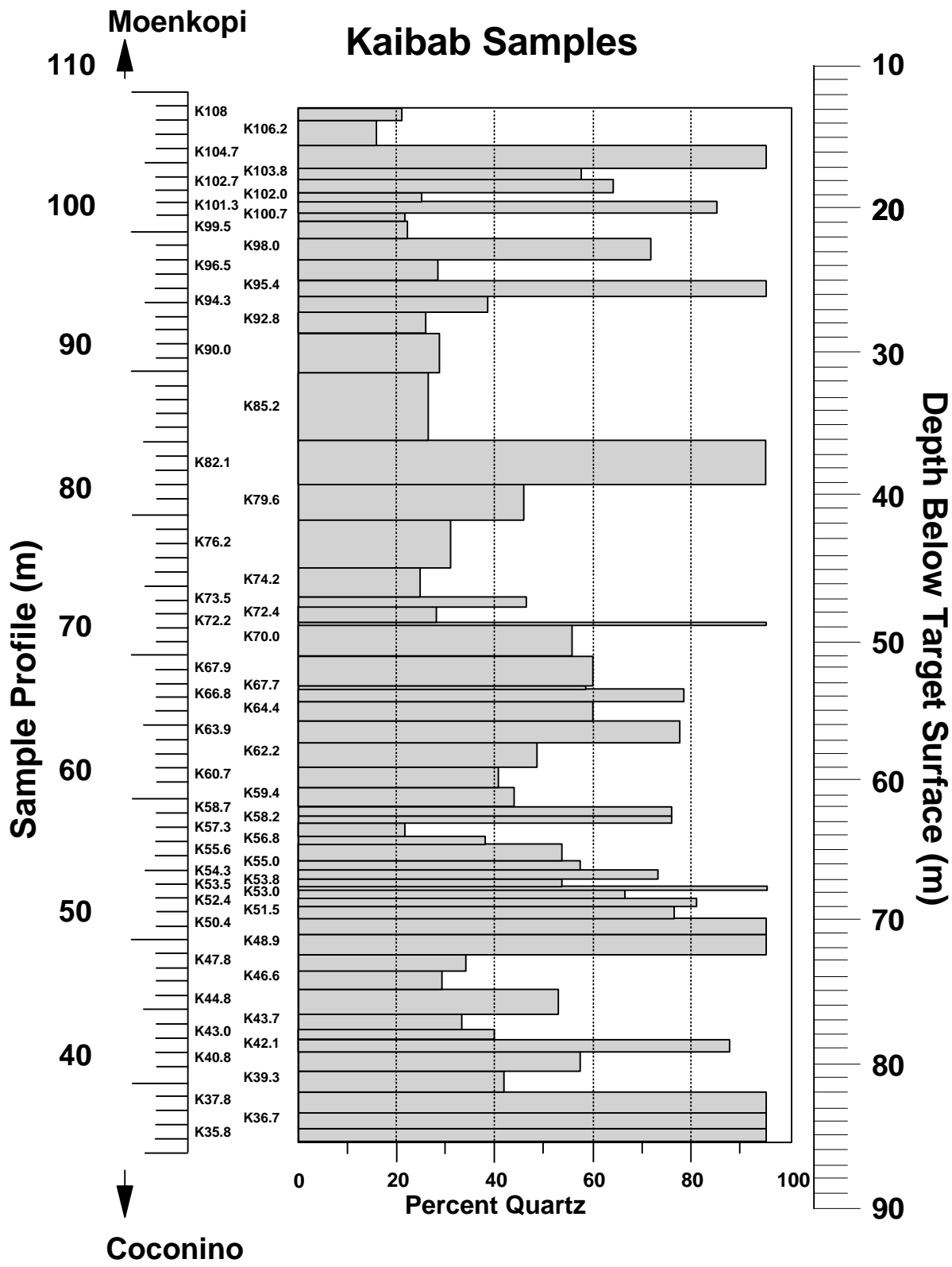


Figure 3. Modal content (wt %) of quartz in the Kaibab Formation at Meteor Crater, AZ, based on XRD studies. The remaining mineral fraction is essentially composed of dolomite.

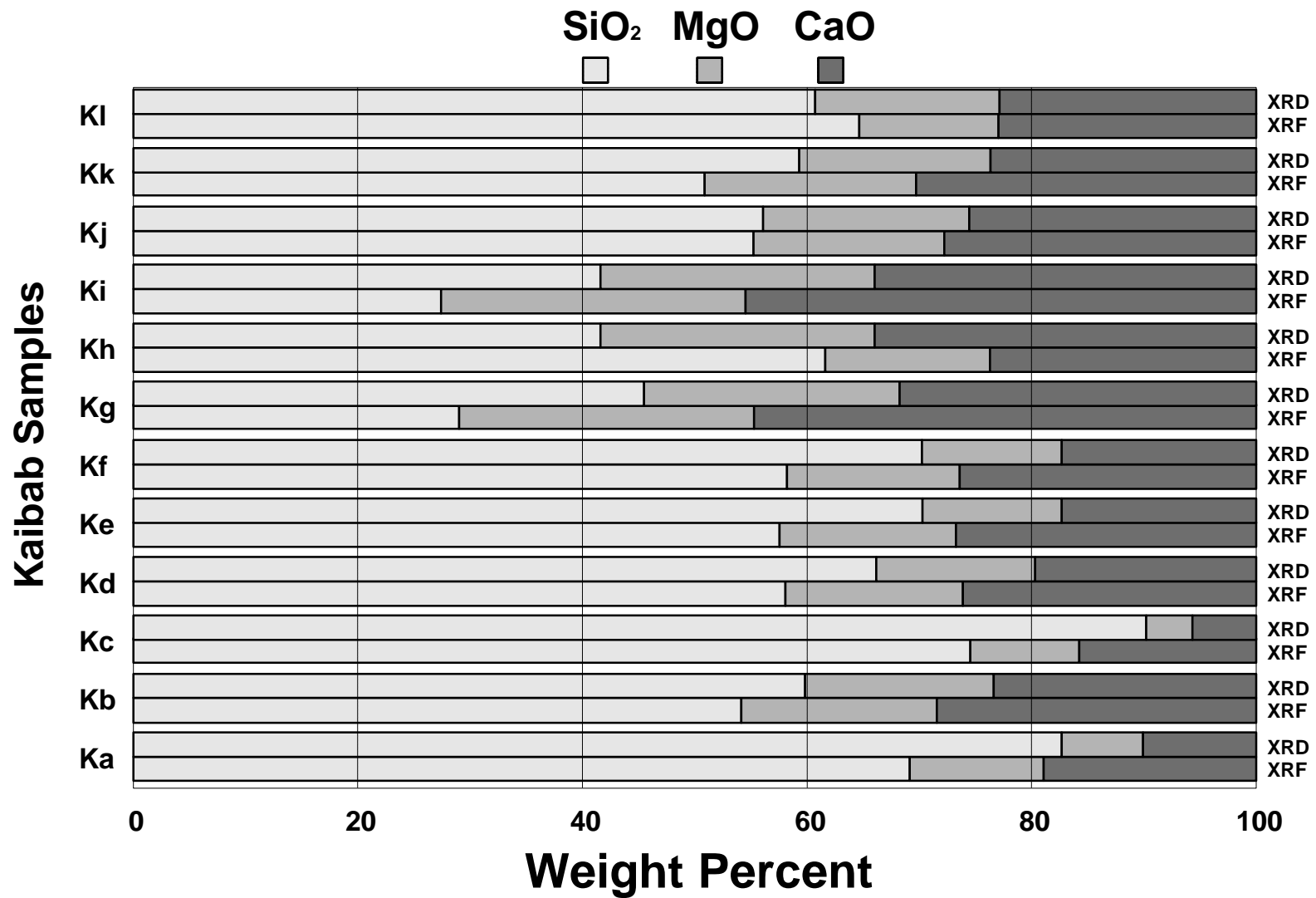


Figure 4. Comparison of the measured SiO₂, MgO, and CaO contents (wt %) of 12 Kaibab subsections based on XRF and comparison with stoichiometric calculations using the modal abundance of quartz and dolomite from XRD. Note that the XRD method tends to modestly overestimate the SiO₂ content in most cases.

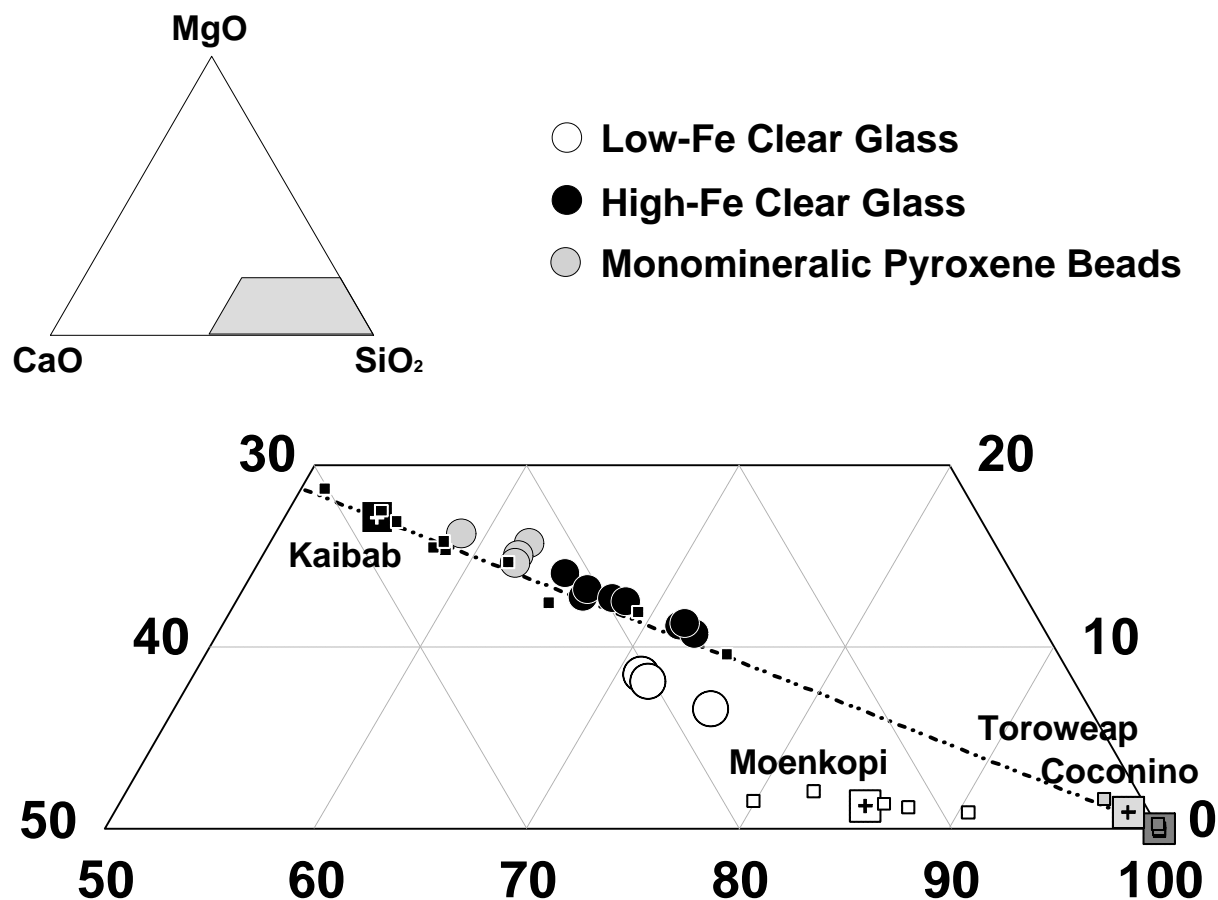


Figure 5. Comparison of the major-element composition of the target rocks and impact melts at Meteor Crater, AZ (from Hörz et al., 2002). For such a direct comparison, only the volatile-free, major minerals (quartz and carbonates) of the target rocks were plotted, and the melt-compositions had to be normalized to a meteorite-free basis. The rocks are represented by squares (large squares are formation averages; small squares are individual subsections; see Table 1); the melts/glasses are represented by circles and classified into 3 specific groups based on their affinity to target rocks, total meteoritic contamination, Fe/Ni ratio and crystallization behavior as detailed by Hörz et al. (2002). Note that the melts at Meteor Crater have highly variable compositions, reflecting different target-provenance and incomplete mixing as detailed in the text.

REPORT DOCUMENTATION PAGE			Form Approved OMB No. 0704-0188	
Public reporting burden for this collection of information is estimated to average 1 hour per response, including the time for reviewing instructions, searching existing data sources, gathering and maintaining the data needed, and completing and reviewing the collection of information. Send comments regarding this burden estimate or any other aspect of this collection of information, including suggestions for reducing this burden, to Washington Headquarters Services, Directorate for Information Operations and Reports, 1215 Jefferson Davis Highway, Suite 1204, Arlington, VA 22202-4302, and to the Office of Management and Budget, Paperwork Reduction Project (0704-0188), Washington, DC 20503.				
1. AGENCY USE ONLY (Leave Blank)	2. REPORT DATE August 2002	3. REPORT TYPE AND DATES COVERED NASA Technical Memorandum		
4. TITLE AND SUBTITLE Major Element Analyses of the Target Rocks at Meteor Crater, Arizona			5. FUNDING NUMBERS	
6. AUTHOR(S) Thomas H. See*, Friedrich Horz, David W. Mittlefehldt, Laura Varley**, Stan Mertzman***, David Roddy****				
7. PERFORMING ORGANIZATION NAME(S) AND ADDRESS(ES) Lyndon B. Johnson Space Center Houston, Texas 77058			8. PERFORMING ORGANIZATION REPORT NUMBERS S-897	
9. SPONSORING/MONITORING AGENCY NAME(S) AND ADDRESS(ES) National Aeronautics and Space Administration Washington, DC 20546-0001			10. SPONSORING/MONITORING AGENCY REPORT NUMBER TM-2002-210787	
11. SUPPLEMENTARY NOTES * Lockheed-Martin Space Operations; ** Lunar and Planetary Institute; *** Franklin & Marshall College; **** United States Geological Survey				
12a. DISTRIBUTION/AVAILABILITY STATEMENT Available from the NASA Center for AeroSpace Information (CASI) 7121 Standard Hanover, MD 21076-1320 Subject Category 42			12b. DISTRIBUTION CODE	
13. ABSTRACT (Maximum 200 words) We collected ~ 400 rock chips in continuous vertical profile at Meteor Crater, Arizona, representing - from bottom to top - the Coconino, Toroweap, Kaibab, and Moenkopi Formations to support ongoing compositional analyses of the impact melts and their stratigraphic source depth(s) and other studies at Meteor Crater that depend on the composition of the target rocks. These rock chips were subsequently pooled into 23 samples for compositional analysis by XRF methods, each sample reflecting a specific stratigraphic "subsection" ~ 5-10 m thick. We determined the modal abundance of quartz, dolomite, and calcite for the entire Kaibab Formation at vertical resolutions of 1-2 meters. The Coconino Formation composes the lower half of the crater cavity. It is an exceptionally pure sandstone. The Toroweap is only 2 m thick and compositionally similar to Coconino; therefore, it is not a good compositional marker horizon. The Kaibab Formation is ~ 80 m thick. XRD studies show that the Kaibab Formation is dominated by dolomite and quartz, albeit in highly variable proportions; calcite is a minor phase at best. The Kaibab at Meteor Crater is therefore a sandy dolomite rather than a limestone, consistent with pronounced facies changes in the Permian of SE Arizona over short vertical and horizontal distances. The Moenkopi forms the 12 m thick cap rock and has the highest Al ₂ O ₃ and FeO concentrations of all target rocks. With several examples, we illustrate how this systematic compositional and modal characterization of the target ideologies may contribute to an understanding of Meteor Crater, such as the depth of its melt zone, and to impact cratering in general, such as				
14. SUBJECT TERMS metamorphism (geology); beds (geology); geology; geomorphology; geophysics;			15. NUMBER OF PAGES 31	16. PRICE CODE
17. SECURITY CLASSIFICATION OF REPORT Unclassified	18. SECURITY CLASSIFICATION OF THIS PAGE Unclassified	19. SECURITY CLASSIFICATION OF ABSTRACT Unclassified	20. LIMITATION OF ABSTRACT Unlimited	
